Scaling of Long-Term Seismicity in Zagros, Iran

Majid Maybodian[1], Mehdi Zare[2*], Hossein Hamzehloo[3], Anoushiravan Ansari[4], and Aref Bali Lashak[5]

1. Ph.D. Candidate, International Institute of Earthquake Engineering and Seismology (IIEES), Iran
2. Associate Professor, Seismological Research Center, International Institute of Earthquake Engineering and Seismology (IIEES), Iran,
* Corresponding Author; email: mzare@iiees.ac.ir
3. Associate Professor, Seismological Research Center, International Institute of Earthquake Engineering and Seismology (IIEES), Iran
4. Assistant Professor, Seismological Research Center, International Institute of Earthquake Engineering and Seismology (IIEES), Iran
5. Assistant Professor, Malek Ashtar University of Technology, Tehran, Iran

Received: 12/10/2012
Accepted: 17/11/2013

ABSTRACT

The long-term Precursory Scale Increase (Ψ) *phenomenon is used to relate minor seismicity to major shallow earthquakes in Zagros. This phenomenon involves an increase in the magnitude and rate of occurrence of minor earthquakes in an area near to the location of a major event. By the modeling of long-term seismogenesis as a three-stage faulting process, the Precursory Scale Increase* (Ψ) *phenomenon can be inferred. Scaling characterizes the parameters of space, time and magnitude that relate the precursory seismicity to the mainshock and aftershocks. Seismogenesis starts with the formation of a major crack, culminates in the corresponding major fracture and earthquake, and ends with healing. Showing high seismicity in south-west of Iran, Zagros mountain accommodate major part of convergence between Arabia and Eurasia. From 1970 to 2009, 29 earthquakes in this region demonstrated a sudden increase in the scale of seismicity, which can be inferred as a long-term precursor. Range of magnitudes of these earthquakes was from 5.6 to 6.7. Precursory time (T_P) interval between onset of the scale increase and occurrence of the earthquake, and the precursory space (A_P) that involved space-time is optimized respectively to scale increase. By scaling relations, predictive regressions are found between the magnitude level of the precursory seismicity (M_P) versus T_P, A_P and the main earthquake magnitude separately. As these relations show high goodness of fit for Zagros, the method could be used in long-range forecasting of the place, time and magnitude of major earthquakes in Zagros region.*

Keywords:
Precursory scale increase; Zagros; Iran; Long-term seismicity

1. Introduction

The most frequently reported precursory phenomena involve patterns of seismicity. Various seismicity patterns before and after major earthquakes have been reported in literature, and therefore several earthquake likelihood models have been published [1]. The seismic cycle is accompanied by the seismic gap hypothesis, first pointed out by Fedotov [2] and then developed by Mogi [3-4]. In a related model, based directly on statistical mechanics, the earthquake is preceded by an accelerating moment release (AMR), which occurs out to radii of several hundred kilometers, and emerges at a highly variable time before the earthquake [5]. Still larger preparation areas are identified by the $M8$ method [6].

On the other hand, many studies, have suggested that seismogenesis is a long-term process, and that the duration of seismicity scales with earthquake magnitude [7]. According to Evison and Rhoades [8], major shallow earthquakes are preceded in the long term by an abrupt scale increase in minor seismicity; this is called the Precursory Scale Increase (Ψ) phenomenon. Compared to M8, the area occupied in each case is small, and the duration of the increase is long. For $M8$, prediction is made separately for each overlapping circles which cover the target territory. The radius of the circles for earthquakes with $M=7$ is 280 km so the investigation area for prediction is about 246,300 km^2 [9]. In this method, the investigation area is chosen according to aftershocks area and is not the same for different regions, but in average it is less than 35,000 km^2 for earthquakes with $M=7$ [8]. Existence of the Ψ phenomenon is an inference from a three-stage model of faulting [10-11], in which the formation of a major crack induces the formation of minor cracks around it. The fracture of the minor cracks prior to that of the major cracks produces the precursory increase in seismicity. From many such examples [12-14], precursory scaling relations were derived, in the form of linear regressions of mainshock magnitude M_m, logarithm of precursor time $\log T_p$, and logarithm of precursory area $\log A_p$ on precursor magnitude M_p. These relations form the basis of the EEPAS model, in which every earthquake is regarded as a precursor, according to scale of larger earthquakes to follow it in the long term. In fact, this study is a retrospective approach to calibrate a set of equations for the intermediate range prediction of earthquakes in Zagros area.

In the Zagros mountain belt, about 50% of the total convergence between Arabia and Eurasia is accommodated [15-16] and is marked by a zone of high seismicity so it could be a good region for testing seismicity scales. The seismicity of earthquakes in Zagros region is studied in this study from 1965 to 2009. For all earthquakes with magnitude more than or equal to 5.5 from 1970 to 2008 (86 earthquakes), Ψ phenomenon is examined, and as a result, 29 out of 86 cases in Zagros show a precursory increase of seismicity or increase of Ψ.

2. Precursory Seismicity

Rising observations show that in subduction regions, there are relations between location, magnitude and time of swarms of minor earthquakes and mainshock [12-14]. Furthermore, observations confirm the similarity of scale between swarms and aftershocks [10-11]. Crack formation before main fracture has been extensively studied in the laboratory [17]. This phenomenon is produced by the growth of a macrocrack and by associated microcracking [18]. The model of this phenomenon was presented by the following way: The possibility of the maincrack and aftercracks generation, increased microearthquake activity at a time preceding the mainshock by years or decades, depending on magnitude. Two elements introduce the length of time interval between crack formation and mainshock caused by cracking. On the one hand the strength is increased with reducing fluid pressure, but on the other hand, the stress-field becomes non-uniform across the major crack and the major crack will not occur until the stress uniformity is obtained [19]. This model can be explained by three-stage faulting: cracking, fracturing, and healing. In this model, both the time before crack formation and the time between crack formation and the major earthquake, is used. Then the phenomenon of the Precursory Scale Increase (Ψ) is introduced, of which the precursory swarm is a special case [8]. The model is quantified by Ψ phenomenon with three parameters: space, time and magnitude. In this respect, the basic element for quantification is the similarity of seismicity increasing before and after mainshock in a given area.

First of all, the precursory area is chosen according to aftershocks and mainshock epicenters, Figure (1a). Second, increasing in seismicity scale is measured by two methods: increasing in magnitude level and increasing in the average rate of seismicity. In this way, the ratio of the average rate of seismicity in the precursory period to the average rate in the prior is measured. For calculating the average rate of seismicity, $C(t)$ is defined as the cumulative magnitude anomaly, Figure (1b), by:

$$C(t) = \sum_{ts<ti<t} (M_i - M_c + 0.1) - k(t - t_s)$$

where (1)

$$k = \sum_{ts<ti<tf} (M_i - M_c + 0.1)/(t_f - t_s) \quad (1)$$

where M_i and t_i are the magnitude and the time of the i^{th} earthquake, respectively. M_c is the threshold magnitude, and k is the average rate of magnitude

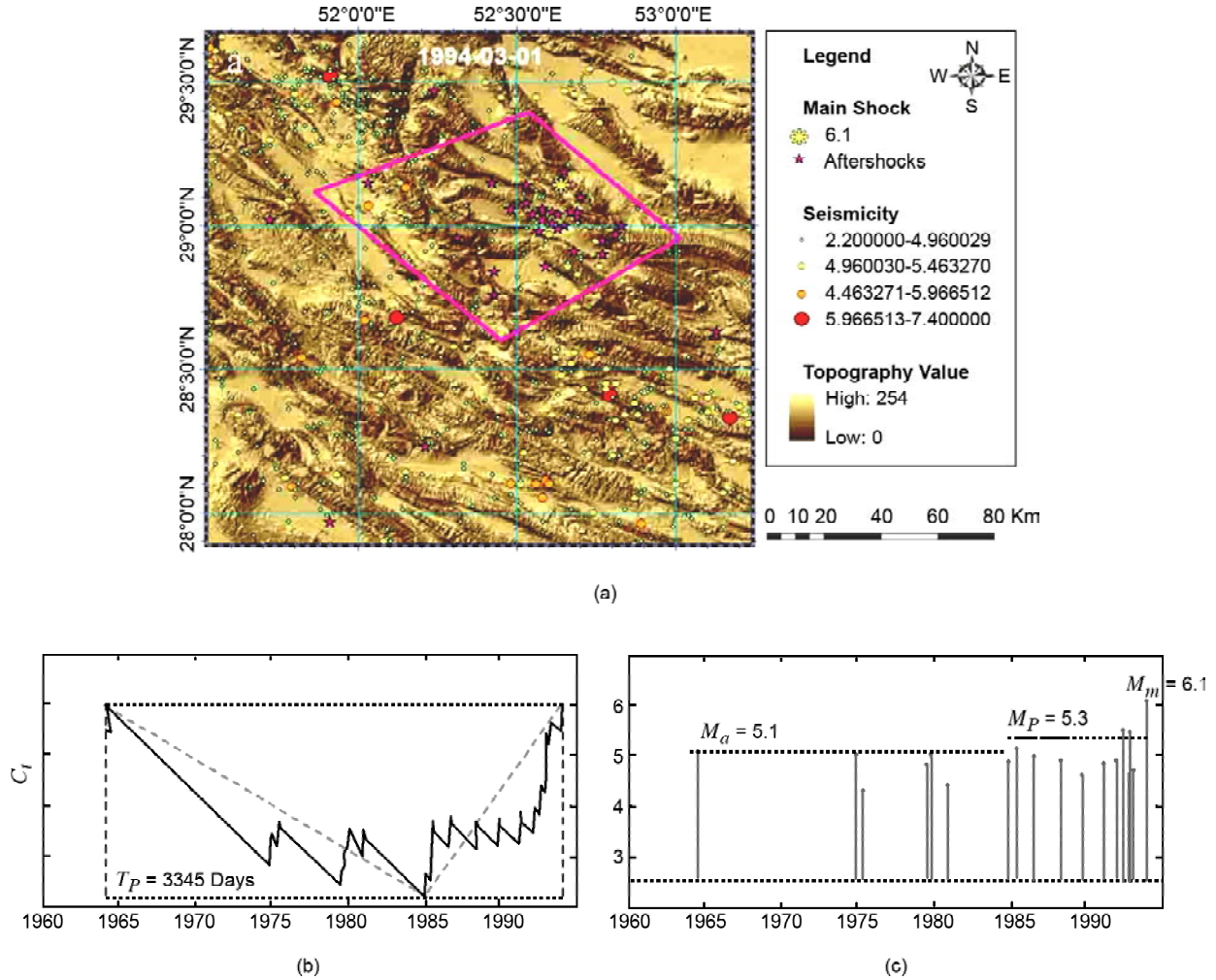

Figure 1. The Ψ phenomenon example shows the following: (a) Epicenters of precursory earthquakes, mainshock and aftershocks. Pink line encloses precursor area A_P. (b) Magnitudes *vs* time of prior and precursory earthquakes, also mainshock and aftershocks. Dashed lines show precursory increase in magnitude level. M_m is mainshock magnitude; M_P is precursor magnitude. (c) Cumag *vs* time.

accumulation between the starting time t_s and the finishing time t_f [11]. A sharp minimum in the $C(t)$ graph is related to a major upward jump in seismicity rate; the low point is taken as the onset of the Ψ anomaly, and the date of the low point marks the start of the precursor time T_P [8].

Third, the increase of seismicity before mainshock (increasing the magnitude level or scale), is calculated by the average of the three largest magnitudes in the set which is named precursory earthquakes, M_P, Figure (1c). The same procedure is done for the magnitude level prior to the scale increase (M_a).

There are three main parameters for the Ψ phenomenon, Figure (1): the magnitude M_P as mentioned above, the time T_P between the start of the precursor and the mainshock, and the area A_P occupied by the precursor, mainshock and aftershocks all scale with mainshock magnitude M_P. Hence M_P could in principle be used to predict the major earthquake via linear regressions of M_m, $\log T_P$ and $\log A_P$ on M_P [20]. These regressions could be presented like:

$$M_m = a_m + b_m M_P \tag{2}$$

$$\log T_P = a_T + b_T M_P \tag{3}$$

$$\log A_P = a_A + b_A M_P \tag{4}$$

where T_P is measured in days, A_P in km^2, and logarithms are to base 10. Evison and Rhoades [8] calculated the precursory relations on 47 examples of the Ψ phenomenon using the earthquake catalogs of California and northern Mexico, Japan, Greece, and New Zealand.

3. Application to Earthquakes in Zagros, Iran

In Zagros region, for all earthquakes with magnitude equal or more than $M_w = 5.5$ (because of having enough aftershocks), the (Ψ) Phenomenon has been investigated. The seismicity of Zagros region (1965-2009) is shown in Figure (2).

In this region, 29 earthquakes from 86 earthquakes with magnitude ≥ 5.5 from 1970 to 2008 have been found with (Ψ) phenomenon, Figure (3) and Aappendix (1). It means, from all of the earthquakes in Zagros region (1970-2008), 29 earthquakes has an increase in both rate and level of seismicity for precursory earthquakes. For all of 86 earthquakes, the precursory area AP has been plotted according to the prior seismicity and aftershock of these main shocks. Unlike the Evison and Rhodes [8], in this study, the area by trend of faults and seismicity of that region is chosen (not a simple NS-EW rectangle). Then the cumulative magnitude anomaly (cumag) $C(t)$ has been tested for all earthquakes, and areas with an increase in the level and rate of seismicity have been chosen for (Ψ) phenomenon. Therefore, we found M_P, T_P and A_P for these earthquakes. After that, the prediction relations for long-range forecasting have been calculated by weighted regression. Accordingly, three parameters are chosen for weighting.

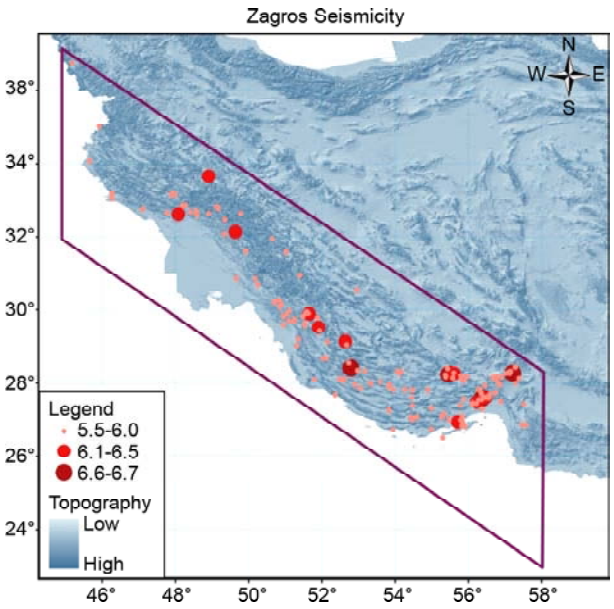

Figure 2. The Zagros region and the seismicity of this region (1965-2009, IIEES catalog) with magnitude ≥ Mw 5.5.

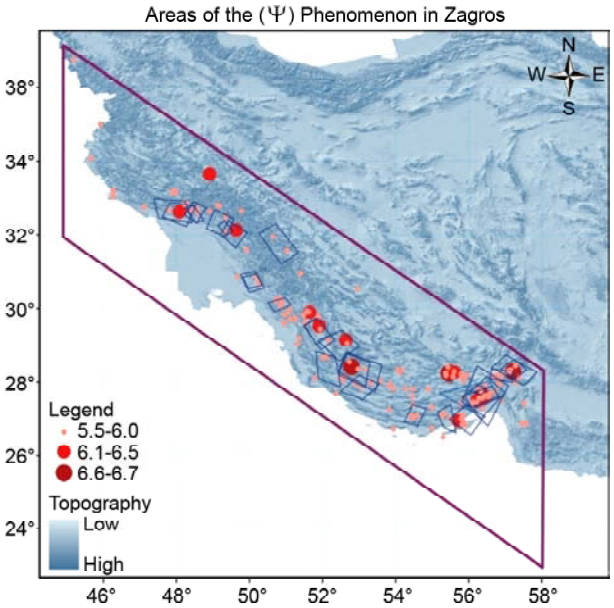

Figure 3. The Areas that show (Ψ) phenomenon (A_P) in Zagros region.

1. Weighting with regards to M_m (w_1).
2. Weighting as for the increase of the scale of magnitude (w_2).
3. Weighting as for the whole time (T_f) of the test (w_3).

The normality assumption is at the core of a majority of standard statistical procedures, and it is important to be able to test this assumption. Among the many procedures used to test this assumption, one of the most well-known procedures is a modification of the Kolmogorov-Smirnov test of goodness of fit, generally referred to as the Lilliefors test for normality [21]. Furthermore, the Durbin-Watson statistic is a test statistic used to detect the presence of autocorrelation (a relationship between values separated from each other by a given time lag) in the residuals (prediction errors) from a regression analysis [22-23]. Durbin and Watson [22-23] applied this statistic to the residuals from least squares regressions, and developed bounds tests for the null hypothesis that the errors are serially independent (not auto correlated) against the alternative that they follow a first order autoregressive process. All of these procedures are done for the seismicity data of Zagros and is shown in Appendix (2).

The relations are in these forms, Figures (4) to (6):

$$M_m = 0.12 + 1.12\, M_P \qquad R^2 = 58\% \tag{5}$$

$$\log T_P = -34.11 + 12.25\, M_P - 1.08 M_P^2 \qquad R2^2 = 47\% \tag{6}$$

$$\log A_P = -3.07 + 0.69\,M_P \quad R2^2 = 64\% \qquad (7)$$

In this research, we used nonlinear regression for T_P–M_P relation (the second order polynomial) to achieve a better goodness of fit.

4. Discussion and Conclusion

In Zagros region, checking the precursory scale increase in seismicity (the Ψ Phenomenon) by means of space-time envelope has shown a strong correlation between the size of the envelope and the earthquake magnitude. Furthermore, by following the trend of faults for precursory areas, better correlation has been achieved compared to previous studies. Despite the calculated relations by Evison and Rhodes [8] in this article the precursory relations

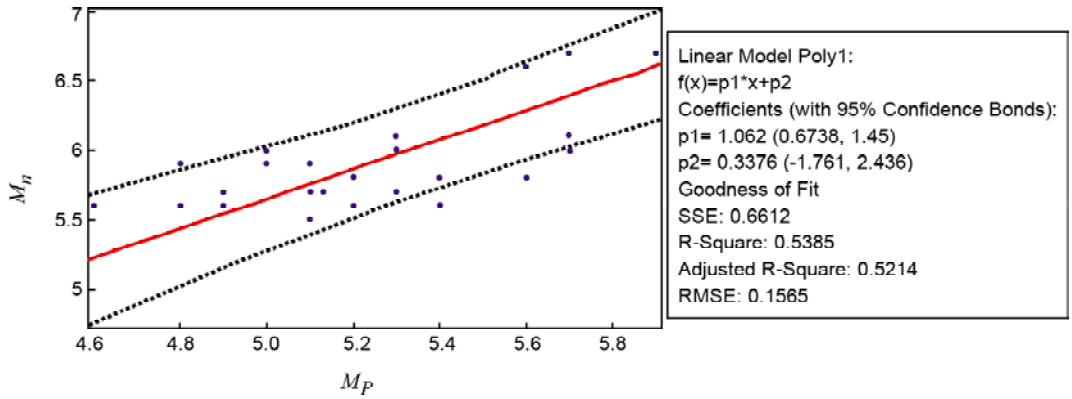

Figure 4. Predictive relation between mainshock magnitude M_m and precursor magnitude M_P, for 29 major earthquakes in Zagros, Dotted lines indicate 95% tolerance limits, Eq. (5).

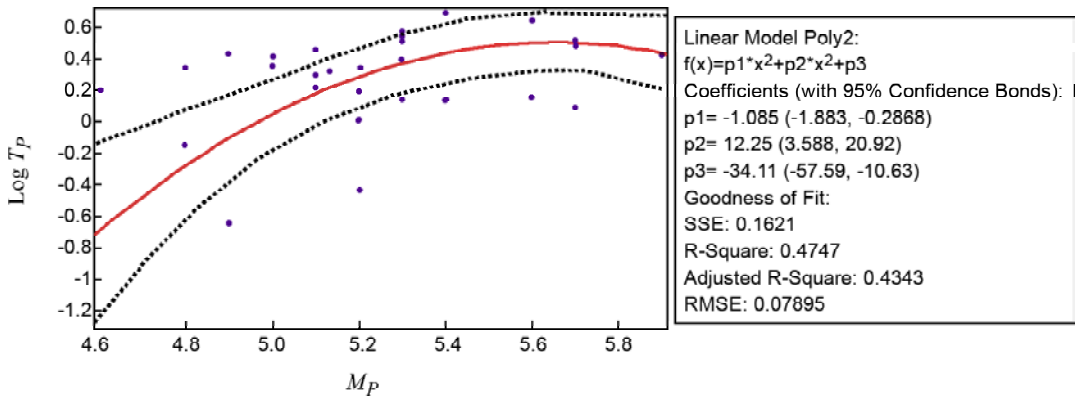

Figure 5. Predictive relation between precursor time T_p and precursor magnitude M_P, for 29 major earthquakes in Zagros, Dotted lines indicate 95% tolerance limits, Eq. (6).

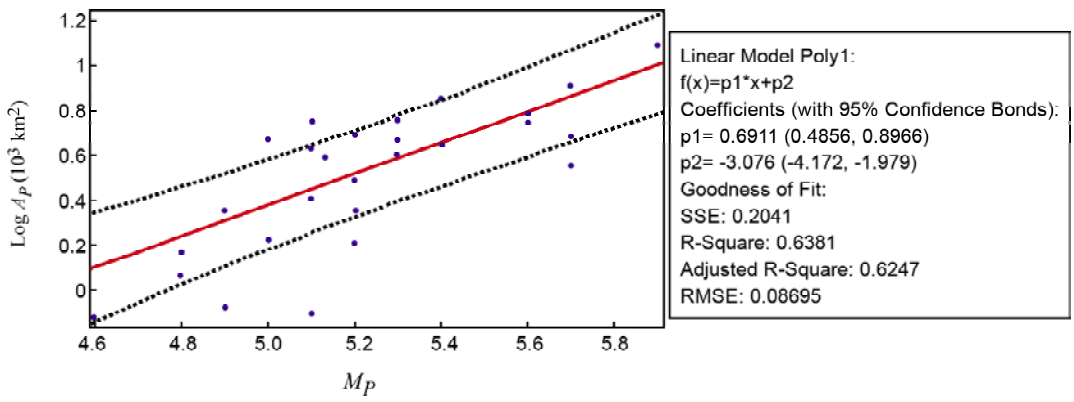

Figure 6. Predictive relation between precursor time A_p and precursor magnitude M_P, for 29 major earthquakes in Zagros, Dotted lines indicate 95% tolerance limits, Eq. (7).

are related for local earthquakes (Zagros, Iran), and these relations could be used for earthquake prediction models as a new function especially in Zagros, Iran.

References

1. Schorlemmer, D., Gerstenberger, M.C., Wiemer, S., Jackson, D.D., and Rhoades, D.A. (2007). Earthquake Likelihood Model Testing, Seismological Research Letters, **78**(1), 17-29.
2. Fedotov, S.A. (1965). On Distribution Patterns for Strong Earthquakes in Kamchatka, the Kurile Islands and Northeastern Japan, Trudy Inst. Fiz. Zemli Akad. Nauk SSSR 36, 66-93.
3. Mogi, K. (1977), Seismic Activity and Earthquake Predictions, Proceedings of the Symposium on Earthquake Prediction, Seis. Soc. Japan, 203-214.
4. Mogi, K. (1985). Earthquake Prediction, Academic Press, Tokyo, 355p.
5. Bowman, D.D., Ouillon, G., Sammis, C.G., Sornette, A., and Sornette, D. (1998). An Observational Test of the Critical Earthquake Concept, *Journal of Geophysical Research*, **103**(B10), 24359-24372.
6. Kossobokov, V.G., Romashkova, L.L., Keylis-Borok, V.I., and Healy, J.H. (1999). Testing Earthquake Prediction Algorithms: Statistically Significant Advance Prediction of the Largest Earthquakes in the Circum-Pacific, 1992-1997, *Physics of the Earth and Planetary Interiors*, **111**(3-4), 187-196.
7. Rikitake, T. (1979). Classification of Earthquake Precursors, *Tectonophysics*, **54**, 293-309.
8. Evison, F.F. and Rhoades, D.A. (2004). Demarcation and Scaling of Long-term Seismogenesis, *Pure Applied Geophysics*, **161**, 21-45.
9. Keilis-Borok, V.I. (1996). Intermediate-Term Earthquake Prediction, *Proceedings of the National Academy of Sciences of the United States of America*, **93**, 3748-3755.
10. Evison, F. and Rhoades, D. (1998). Long-Term Seismogenic Process for Major Earthquakes in Subduction Zones, *Physics of the Earth and Planetary Interiors*, **108**, 185-199.
11. Evison, F.F. and Rhoades, D.A. (2001). Model of Long-Term Seismogenesis, *Annals of Geofysics*, **44**(1), 81-93.
12. Evison, F.F. and Rhoades, D.A. (1997), The Precursory Earthquake Swarm in New Zealand: Hypothesis Tests, II, *New Zealand Journal of Geology and Geophysics*, **40**, 537-547.
13. Evison, F.F. and Rhoades, D.A. (1999). The Precursory Earthquake Swarm in Japan: Hypothesis Test, *Earth, Planets and Space*, **51**(12), 1267-1277.
14. Evison, F.F. and Rhoades, D.A. (2000). The Precursory Earthquake Swarm in Greece, *Annali di Geofisica*, **43**, 991-1009.
15. Tatar, M., Hatzfeld, D., Martinod, J., Walpersdorf, A., Ghafory-Ashtiany, M., and Chery, J. (2002). The Present-Day Deformation of Central Zagros from GPS Measurements, *Geophysical Research Letters*, **29**, doi: 10.1029/2002GL015427.
16. Vernant, P. et al. (2004). Present Day Crustal Deformation and Plate Kinematics in the Middle East Constrained by GPS Measurements in Iran and Northern Oman, *Geophysical Journal International*, **157**, 381-398.
17. Scholz, C.H. (1990). The Mechanics of Earthquakes and Faulting, Cambridge University Press, Cambridge, 21p.
18. Atkinson, B.K. and Rawlings, R.D. (1981). Acoustic Emission during Stress Corrosion Cracking in Rocks, Earthquake Prediction: an International Review (American Geophysical Union, Washington, D.C.), 605-616.
19. Mogi, K. (1963). Some Discussions on Aftershocks, Foreshocks and Earthquake Swarms - the Facture of a Semi-Infinite Body Caused by an Inner Stress Origin and Its Relation to the Earthquake Phenomena, Bulletin of the Earthquake Research Institute, **41**(3), 615-658.
20. Rhoades, D.A. and Evison, F.F. (2006). The EEPAS Forecasting Model and the Probability of Moderate-to-Large Earthquakes in Central Japan, *Tectonophysics*, **417**, 119-130
21. Lilliefors, H.W. (1967). On the Kolmogorov-Smirnov Test for Normality with Mean and

Variance Unknown, *Journal of the American Statistical Association*, **62**, 399-402.

22. Durbin, J. and Watson, G.S. (1950). Testing for Serial Correlation in Least Squares Regression, I, *Biometrika*, **37**, 409-428.

23. Durbin, J. and Watson, G.S. (1951). Testing for Serial Correlation in Least Squares Regression, II, *Biometrika*, **38**, 159-179.

Appendix I

Table 1. Earthquakes showing (Ψ) phenomenon in Zagros from 1970 to 2008.

	Year	Month	Day	M_m	M	M_p	T_p (Day)	A_p (Km^2)	T_f (Year)
1	1970	2	28	5.7	4.8	5.1	2098	3942	10
2	1971	11	8	5.9	5.09	5.1	2863	2545	10
3	1971	12	9	5.8	5	5.4	1374	7193	12
4	1972	4	3	5.7	4.4	5.3	3198	4698	12
5	1972	4	10	6.7	4.4	5.7	3205	8244	12
6	1972	7	2	5.6	4.8	5.2	367	1594	4
7	1976	4	22	6	4.9	5.0	2212	4665	13
8	1977	3	21	6.7	5.3	5.9	2636	12279	17
9	1977	4	6	6	5	5.3	1376	4670	17
10	1977	5	19	5.8	4.9	5.2	1539	2273	17
11	1977	6	5	6.1	4.8	5.1	1650	4243	13
12	1978	12	14	6.2	5	5.2	2169	3076	14
13	1982	7	11	5.5	4.3	5.1	1986	783	9
14	1983	3	5	5.7	5	5.3	3715	3954	19
15	1983	5	28	5.8	5.4	5.6	1428	6069	19.5
16	1983	7	12	6	5.3	5.7	3082	3635	19.5
17	1985	8	7	5.6	5.2	5.4	4932	4520	24
18	1988	3	30	5.9	4.7	4.8	700	1465	23
19	1988	8	11	6.1	5.6	5.7	1226	4856	11
20	1989	4	2	5.7	5	5.1	1952	5692	29
21	1994	3	1	6.1	5.1	5.3	3346	5748	20
22	1994	7	31	5.6	4.79	4.8	2191	1167	2
23	1997	10	20	5.7	4.7	4.9	230	2283	24
24	1999	3	4	6.6	5.3	5.6	4384	5637	34
25	1999	5	6	6.3	5.2	5.3	2471	4040	29
26	2000	3	5	5.6	4.5	4.6	1590	759	12
27	2002	9	25	5.6	4.89	4.9	2700	842	37
28	2006	2	28	5.9	4.99	5.0	2583	1662	18
29	2008	9	10	6.2	4.8	5.2	1017	4897	3

Appendix II

Table 2. The results of different regression and the analysis of the regression for the Zagros seismicity precursory relations.

		$Y= a + bx + Cx^2$						
Parameters	Regression type	a	b	c	R^2 (%)	h*	d**	Comments
M_m - M_p	Simple	2.46	0.66	0	38	0	1.79	
M_m - M_p	Weighted- Sum/Max: (w1+w2+w3)/Max	1.82	0.79	0	44	0	1.64	
M_m - M_p	Weighted- Sum/Max: (w1+w3)/Max	2.13	0.73	0	42	0	1.45	
M_m - M_p	Weighted- Sum/Max: (w1+w2)/Max	1.60	0.83	0	45	0	1.81	

Table 2. Continue.

		$Y= a + bx + Cx^2$						
Parameters	Regression type	a	b	c	R^2 (%)	h*	d**	Comments
M_m - M_p	Weighted- Sum/Max: (w2+w3)/Max	1.62	0.82	0	45	0	1.74	
M_m - M_p	Weighted- Sum: (w1+w2+w3)	2.25	0.70	0	40	0	1.48	
M_m - M_p	Weighted- Sum: (w1+w3)	2.28	0.70	0	39	0	1.47	
M_m - M_p	Weighted- Sum: (w1+w2)	1.50	0.85	0	46	0	1.87	
M_m - M_p	Weighted- Sum: (w2+w3)	2.26	0.70	0	40	0	1.48	
M_m - M_p	Weighted- Multiple: (w1.*w2.*w3)	0.28	1.09	0	57	1	1.77	
M_m - M_p	Weighted- Multiple: (w1.*w3)	1.91	0.79	0	45	0	1.23	
M_m - M_p	Weighted- Multiple: (w1.*w2)	0.12	1.12	0	58	1	2.12	chosen
M_m - M_p	Weighted- Multiple: (w2.*w3)	0.34	1.06	0	54	0	1.75	
M_m - M_p	w1	2.11	0.75	0	43	0	1.50	
M_m - M_p	w2	-0.04	1.13	0	56	0	2.23	
M_m - M_p	w3	2.30	0.70	0	39	0	1.48	
				0				
T_P - M_p	Simple	-1.36	0.31	0	10.5	1	2.42	
T_P - M_p	Weighted- Sum/Max: (w1+w2+w3)/Max	-1.78	0.39	0	18	1	2.39	
T_P - M_p	Weighted- Sum/Max: (w1+w3)/Max	-1.70	0.38	0	17	1	2.36	
T_P - M_p	Weighted- Sum/Max: (w1+w2)/Max	-1.76	0.38	0	19	1	2.39	
T_P - M_p	Weighted- Sum/Max: (w2 +w3)/Max	-1.96	0.43	0	19	0	2.34	
T_P - M_p	Weighted- Sum: (w1+w2+w3)	-1.93	0.42	0	18	0	2.28	
T_P - M_p	Weighted- Sum: (w1 +w3)	-1.92	0.42	0	18	0	2.28	
T_P - M_p	Weighted- Sum: (w1+w2)	-1.80	0.39	0	19	1	2.39	
T_P - M_p	Weighted- Sum: (w2+w3)	-1.94	0.43	0	19	0	2.28	
T_P - M_p	Weighted- Multiple: (w1.*w2.*w3)	-2.24	0.48	0	32	1	2.38	
T_P - M_p	Weighted- Multiple: (w1.*w3)	-2.08	0.45	0	25	0	2.35	
T_P - M_p	Weighted- Multiple: (w1.*w2)	-2.26	0.47	0	32	1	2.02	
T_P - M_p	Weighted- Multiple: (w2.*w3)	-2.45	0.52	0	29	1	2.44	
T_P - M_p	w1	-1.58	0.35	0	17	1	2.33	
T_P - M_p	w2	-2.31	0.49	0	24	1	2.20	
T_P - M_p	w3	-1.94	0.43	0	18	0	2.27	
T_P - M_p	Simple	-4.89	1.66	-0.13	11	1	2.42	
T_P - M_p	Weighted- Sum/Max: (w1+w2+w3)/Max	-12.86	4.57	-0.39	20	1	2.39	
T_P - M_p	Weighted- Sum/Max: (w1 +w3)/Max	-13.69	4.91	-0.42	20	0	2.36	
T_P - M_p	Weighted- Sum/Max: (w1 +w2)/Max	-11.61	4.07	-0.34	20	1	2.45	
T_P - M_p	Weighted- Sum/Max: (w2 +w3)/Max	-13.48	4.78	-041	22	1	2.30	
T_P - M_p	Weighted- Sum: (w1+w2+w3)	-15.87	5.72	-0.50	22	0	2.22	
T_P - M_p	Weighted- Sum: (w1 +w3)	-16.04	5.80	-0.51	22	0	2.22	
T_P - M_p	Weighted- Sum: (w1 +w2)	-11.95	4.16	-0.35	22	1	2.43	
T_P - M_p	Weighted- Sum: (w2 +w3)	-15.94	5.75	-0.50	22	0	2.22	
T_P - M_p	Weighted- Multiple: (w1.*w2.*w3)	-34.11	12.25	-1.08	47	1	2.57	chosen
T_P - M_p	Weighted- Multiple: (w1.*w3)	-23.15	8.38	-0.74	33	1	2.49	
T_P - M_p	Weighted- Multiple: (w1.*w2)	-22.88	8.08	-0.70	38	1	2.07	
T_P - M_p	Weighted- Multiple: (w2.*w3)	-28.73	10.31	-0.91	40	1	2.50	
T_P - M_p	w1	-11.72	4.16	-0.36	19	1	2.38	
T_P - M_p	w2	-14.67	5.08	-0.43	26	1	2.25	
T_P - M_p	w3	-16.11	5.81	-0.51	22	0	2.21	

Table 2. Continue.

		$Y = a + bx + Cx^2$						
Parameters	Regression type	a	b	c	R^2 (%)	h*	d**	Comments
T_P - M_p	Simple	-3.59	0.78	0	59	0	2.11	
A_P - M_p	Weighted- Sum/Max: (w1+w2+w3)/Max	-3.4	0.75	0	60	0	1.92	
A_P - M_p	Weighted- Sum/Max: (w1 +w3)/Max	-3.32	0.73	0	61	0	1.84	
A_P - M_p	Weighted- Sum/Max: (w1 +w2)/Max	-3.27	0.73	0	58	0	2.01	
A_P - M_p	Weighted- Sum/Max: (w2 +w3)/Max	-3.66	0.79	0	59	0	1.93	
A_P - M_p	Weighted- Sum: (w1+w2+w3)	-3.57	0.78	0	60	1	1.78	
A_P - M_p	Weighted- Sum: (w1+w3)	-3.56	0.78	0	60	1	1.77	
A_P - M_p	Weighted- Sum: (w1+w2)	-3.31	0.73	0	58	0	2.00	
A_P - M_p	Weighted- Sum: (w2+w3)	-3.57	0.78	0	60	1	1.78	
A_P - M_p	Weighted- Multiple: (w1.*w2.*w3)	-3.04	0.69	0	65	1	1.81	
A_P - M_p	Weighted- Multiple: (w1.*w3)	-3.07	0.69	0	64	0	1.71	Chosen
A_P - M_p	Weighted- Multiple: (w1.*w2)	-3.17	0.71	0	62	1	1.76	
A_P - M_p	Weighted- Multiple: (w2.*w3)	-3.39	0.74	0	57	1	1.92	
A_P - M_p	w1	-3.06	0.69	0	61	0	2.01	
A_P - M_p	w2	-3.94	0.85	0	56	1	1.97	
A_P - M_p	w3	-3.57	0.78	0	60	1	1.77	